Supporting Material for

Interleukin-10 from CD4$^+$ follicular regulatory T cells promotes the germinal center response

Brian J. Laidlaw[1,2,6], Yisi Lu[1,6], Robert A. Amezquita[1], Jason S. Weinstein[5], Jason A. Vander Heiden[4], Namita T. Gupta[4], Steven H. Kleinstein[1,3,4], Susan M. Kaech[1], and Joe Craft[,1,5]

Correspondence should be addressed to JC (joseph.craft@yale.edu)

This PDF includes

SUPPLEMENTAL METHODS

Antibodies for surface and intracellular staining. The isolation of lymphocytes, along with surface and intracellular staining, was performed as described (*57*). Staining of transcription factors was performed after permabilization with the Foxp3 Fixation and Permeabilization Kit (eBioscience). Intracellular phosphorylated (p) p-Akt^{S473} and p-S6$^{235/236}$ were detected via paraformaldehyde fixation and methanol permeabilization and antibodies from Cell Signaling. Primary unconjugated antibodies used in phospho-flow were detected by secondary staining with anti-rabbit IgG 647 antibody (Molecular Probes). Staining of BRDU was performed with the FITC BRDU flow kit (BD Biosciences, 559619) following manufacturer's instructions. For phospho-Stat3 staining, the cells were stimulated with IL-10 (100μg/ml) for 30 minutes at 37 degrees Celsius and then underwent fixation with 4% paraformaldehyde and permeabilization with methanol before staining. Nuclear FOXO1 localization was performed following IL-10 stimulation with Amnis Imagestream and analyzed with Imagestream IDEAS software (EMD Millipore). The following antibodies were used for flow cytometry staining: Brilliant Violet 605 anti-CXCR5 (145513), allophycocyanin(APC)–anti-KLRG1 (138412), phycoerythrin (PE)–indotricarbocyanine (Cy7)–anti-CD69 (104512), peridinin chlorophyll protein (PerCP)–anti-Thy-1.1 (202512), Pacific Blue–conjugated antibody to major histocompatibility complex class II (107619), fluorescein isothiocyanate (FITC)–anti-Ly6C (128022), PE-Cy7-anti-PD-1 (109110), Brilliant Violet 510-anti-CD4 (100559), Pacific Blue-anti-CD38 (102720), PerCP-Cy5.5-anti-IgM (406512) and PE-Cy7-anti-CD11c (117318) (all from BioLegend); allophycocyanin-Cy7 (APC-Cy7)-anti-CD44 (47-0042-82), APC-anti-CXCR4 (17-9991-82), Biotin-anti-GL7 (13-5902-82), eFluor 450-anti-IgD (48-5993-82), PE-anti-CTLA-4 (12-1522-82), APC-anti-Foxp3 (17-5773-82) and PE–anti-CD25 (12-0251-83) (all from eBioscience); Pacific Blue-anti-CD4 (558107), PE-CF954-anti-B220 (562290), PE-Cy7-anti-CD95 (557653), FITC-anti-GL7 (553666), FITC–anti-CD62L (553150) and PE–anti-CD86 (553692), PE-anti-Bcl6 (561522), Brilliant violet-421-anti-Psgl1 (562807), APC-anti-CD138 (561705) and Biotin-anti-IgG2a (553504) (all from BD Biosciences); rabbit mAb to phospho-Stat3 (9131S) and rabbit mAb to Foxo1 (2880S) (both from Cell Signaling). Major histocompatibility complex class II tetramers were generated as previously described (*58*). Flow cytometry data were acquired on a BD LSRII with FACSDiva software and were analyzed with FlowJo software (TreeStar).

Isolation of lymphocytes from tissues. Spleens were homogenized with a cell strainer, and red blood cells were lysed with ACK lysing buffer (Quality Biologicals). Peripheral and mesenteric lymph nodes, as well as peyer's patches were isolated and homogenized with the coarse side from microscopic slides. Lymphocytes were then washed and counted.

Confocal imaging. Spleens were prepared by overnight fixation at 4 °C with periodate-lysine-paraformaldehyde (PLP) buffer (50mM phosphate buffer, 0.1M L-Lysine (Sigma), 1% paraformaldehyde (Sigma) and 0.2% sodium M-periodate (Sigma)). The fixed spleens were frozen in 100% optimum cutting temperature (O.C.T.) compound (VWR) in cryomolds and stored at -80°C. The frozen tissues were cut into 8 μm sections and processed as previously described (*33*).The sections were stained with FITC-anti-IgD (553439) from BD Bioscience, biotin-anti-PNA (B-1075) from Vector Lab and Streptavidin-Alexa 555 (S-32355) from Invitrogen. Images were acquired on a Leica TCS SP5 Spectral Confocal Microscope with the objective at 40x magnification. ImageJ was used to quantify the size of GCs.

ELISA for LCMV-specific antibodies. 96-polysorp microtiter plates (Nunc) were coated overnight with cell lysates from LCMV-infected BHK-21 cells as described (*58*). Alkaline phosphatase (AP)-conjugated goat anti-mouse IgG1 and IgG2a (Southern Biotech) were used to detect antibody of specific isotypes to LCMV. Relative units were extrapolated based on the ODs using Softmax Pro 3.1 software (Molecular Devices).

ELISPOT for LCMV-specific memory B cells. MultiScreen HTS plates (Millipore) were coated overnight with cell lysates from LCMV-infected BHK-21 cells as described (*58*). 100,000 B cells isolated using the EasySep Mouse B cell isolation kit (StemCell Technologies) were added to each well the following day in triplicate with or without LPS (5 μg/ml). Cells were cultured for 5 days and then stained with Alkaline phosphatase (AP)-conjugated goat anti-mouse IgG1 and IgG2a (Southern Biotech). Spots were developed with Vector Blue (Vector Laboratories), and quantified using an ImmunoSpot analyzer (Cellular Technology Limited).

RNA-seq library preparation and data analysis. Total RNA was purified with the use of a Qiazol and RNeasy Mini kit (Qiagen), in which on-column treatment with DNase was included. Purified RNA was submitted to the Yale Center for Genomic Analysis, where it was subjected to isolation of mRNA and library preparation. Libraries were pooled, six samples per lane, and were sequenced on an Illumina HISEQ 2500 (75–base pair paired-end reads), followed by alignment with STAR (*59*). A 'count-based' differential-expression protocol was adapted for this analysis (*59*). Mappable reads were counted with HTseq and imported into R software for analysis of differential expression with DESeq2 software. A multi-factor design was used to take into the two conditions (*Il10*$^{f/f}$*Foxp3*-Cre and *Il10*$^{f/f}$) and account for pairwise groupings of the six samples. For the generation of the heat map, genes with a difference in expression (log2) of 1.5-fold or greater and a false-discovery rate of <0.1 were chosen for visualization of

the over- all consensus of rankings (via column z-score). Select biologically relevant genes were chosen for a subsequent presentation on a heat map.

Cloning and sequencing of GC B cells. GC B cells were harvested from spleens of mice infected with LCMV Armstrong 15 days p.i. RNA was isolated from 2-4 × 10^5 sorted GC B cells and cDNA was synthesized using iScript cDNA Synthesis Kit (Bio Rad). Isotype-specific reverse transcription-PCR using Phusion high-fidelity Taq (Finnzymes) were performed to amplify the immunoglobulin heavy-chain variable region (VH) repertoire as previously described to obtain a "global" picture of the immunoglobulin genes (*60*). Specifically, the cDNAs were amplified by using a combination of eight different forward primers (VHF1-8) targeted to the mouse V regions and a reverse primer (VHR2) specific for all mouse J regions (*47*, *61*). The PCR products were cloned into pCR-Blunt vector by zero blunt TOPO cloning (Invitrogen). Single colonies were selected for DNA sequence analysis using Applied Biosystems 3730 capillary instrument. Unique sequences matching the V_H genes were analyzed using IgBLAST (*62*).

GC B cell sequence analysis. . Germline gene segments (V_H, D_H, and J_H) for the IgH variable region sequences were inferred using IMGT/HighV-QUEST (*63*). The extent of somatic mutation was evaluated relative to the alignment provided by the IMGT/HighV-QUEST, using the Change-O commandline rools (*64*)for processing and the ShazaM R package (*64*, *65*) for the quantification and comparison of selection pressures. These analyses were conducted as previously described (*66*, *67*). Physiochemical properties were analyzed using the Alakazam R package (*48*, *64*).

Gene Set Enrichment Analysis (GSEA). Gene sets from the Broad Molecular Signatures Database and other published data sets (*6*, *41*) were chosen for assessment of enrichment in the RNA-seq analysis of *Il10*$^{f/f}$*Foxp3*-Cre versus *Il10*$^{f/}$f RNA-seq. R-GSEA code was used for analysis of the data, with the signal-to-noise ranking metric and 1 × 10^5 permutations of the gene labels for testing of statistical significance using the false discovery rate (Benjamini-Hochberg) cutoff of 0.001 for significance, and the family-wise error rate (FWER) was calculated for visualization of result. Results were visualized with R, with the running enrichment score, member position by the signal-to-noise ranking metric ('bar code'), and ranking metric scale presented. Values in gene-set plots showing individual differences in expression (log2) ± standard error were derived from analysis of the RNA-seq data with DESeq2 software (*68*). Normalized enrichment scores were adjusted by the family wise-error rate (FWER) to correct for false-positive gene set.

Pathway Analysis. The pathway analysis was performed using the Ingenuity Pathway Analysis software (Qiagen). The Canonical pathway analysis was conducted across the *Il10*$^{f/f}$*Foxp3*-Cre versus *Il10*$^{f/f}$ RNA-seq dataset; the significance values (log p value) were calculated by Benjamini-Hochberg procedure. The Upstream analysis was performed to identify upstream regulators across the *Il10*$^{f/f}$*Foxp3*-Cre and *Il10*$^{f/f}$ dataset based on predictions made by the z-score algorithm (www.ingenuity.com).

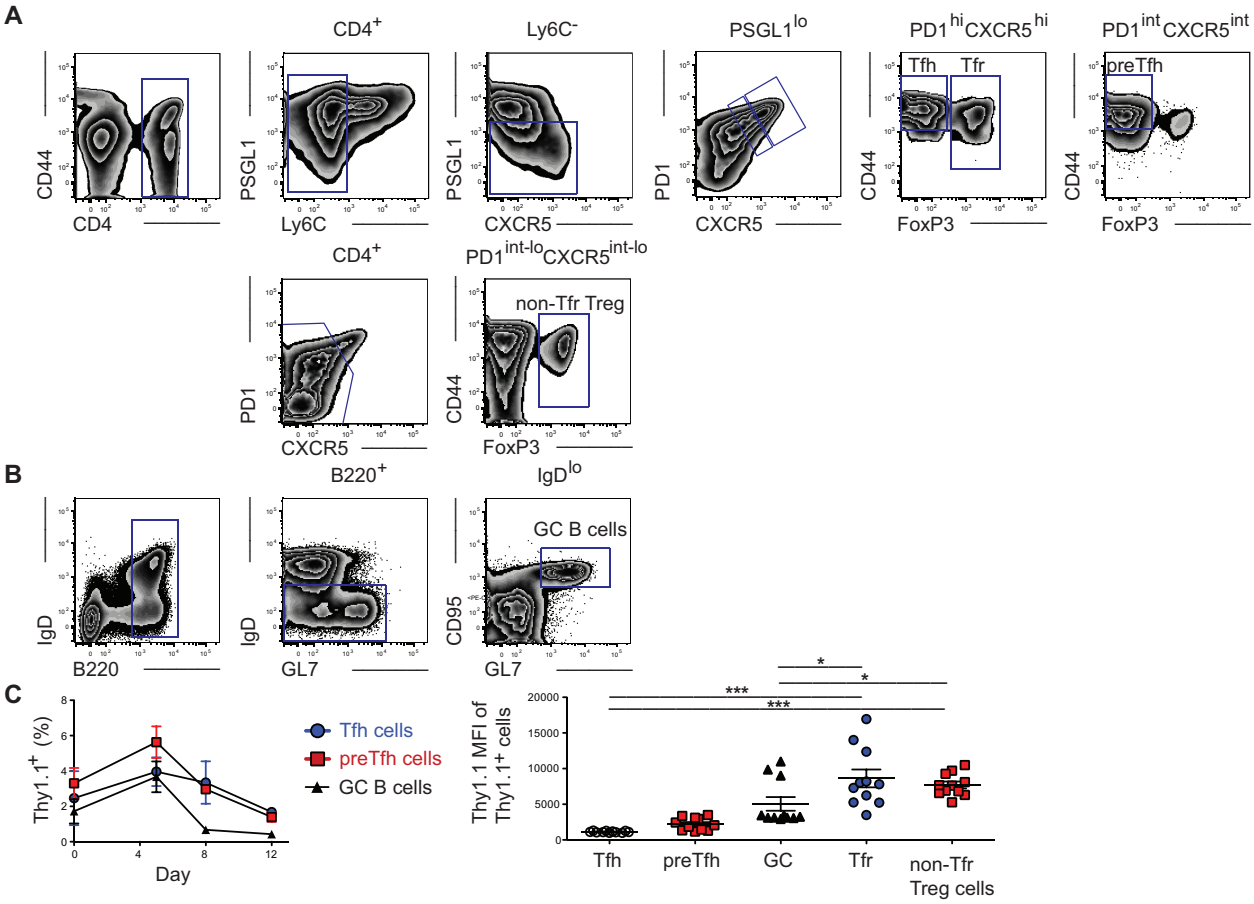

Figure S1. Flow cytometric gating strategy for Tfh, pre-Tfh, GC B, Treg, and Tfr cells, with IL-10 expression by these populations. (a) T cell populations are defined as follows: Tfr cells: $CD4^{+}Ly6C^{-}PSGL1^{lo}CXCR5^{hi}PD1^{hi}Foxp3^{+}$, non-Tfr Treg cells: $CD4^{+}CXCR5^{int\text{-}lo}PD1^{int\text{-}lo}Foxp3^{+}$, pre-Tfh cells: $CD4^{+}Ly6C^{-}PSGL1^{lo}CXCR5^{int}PD1^{int}Foxp3^{-}CD44^{hi}$, Tfh cells: $CD4^{+}Ly6C^{-}PSGL1^{lo}CXCR5^{hi}PD1^{hi}Foxp3^{-}CD44^{hi}$. Gating was performed such that no assumptions were made regarding the expression of CD44 on Tfr or Non-Tfr Treg cells. (**b**) GC B cells were defined as $B220^{+}IgD^{lo}GL7^{+}CD95^{+}$. (**c**) Frequency of IL-10 competent (Thy-1.1^{+}) cells among Tfh, preTfh, and GC B populations at days 0, 5, 8, and 12 following LCMV Armstrong infection (left). Thy1.1 MFI of Thy-1.1^{+} cells among Tfh, preTfh, GC B, Tfr, and non-Tfr Treg populations (right) pooled from day 5, 8, and 12 p.i. Data are from 1 experiment representative of 4 experiments with 3-6 mice per time point post LCMV Armstrong infection. Statistical analyses were performed using the unpaired two-tailed Student's *t*-test. (*, $p < 0.05$; ***, $p < 0.001$).

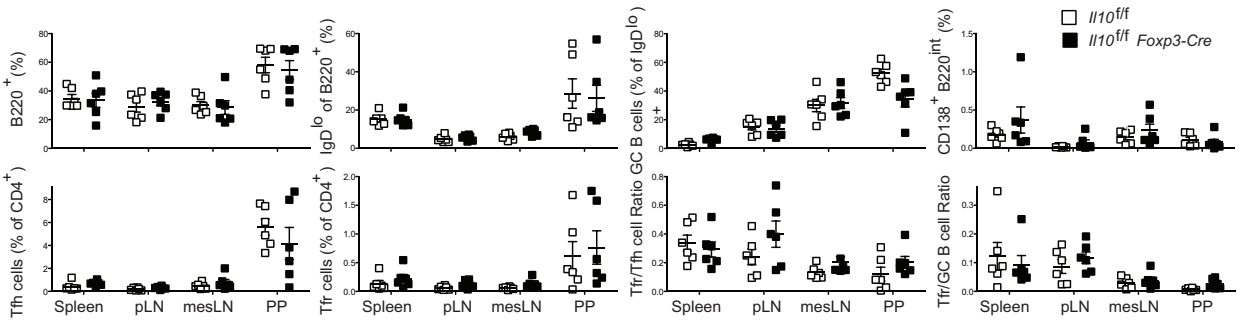

Figure S2. Mice lacking regulatory CD4$^+$ T cell-derived IL-10 do not have defects in steady state lymphoid cell populations. Analysis of the B cell, CD138$^+$ B220^{int} plasmablast, Tfh, and Tfr cell responses in the spleen, peripheral lymph nodes (pLNs), mesenteric lymph nodes (mesLN), and Peyer's patches (PP) of uninfected *Il10*$^{f/f}$ and *Il10*$^{f/f}$ *Foxp3*-Cre mice. Data are pooled from two independent experiments with 3 mice per group.

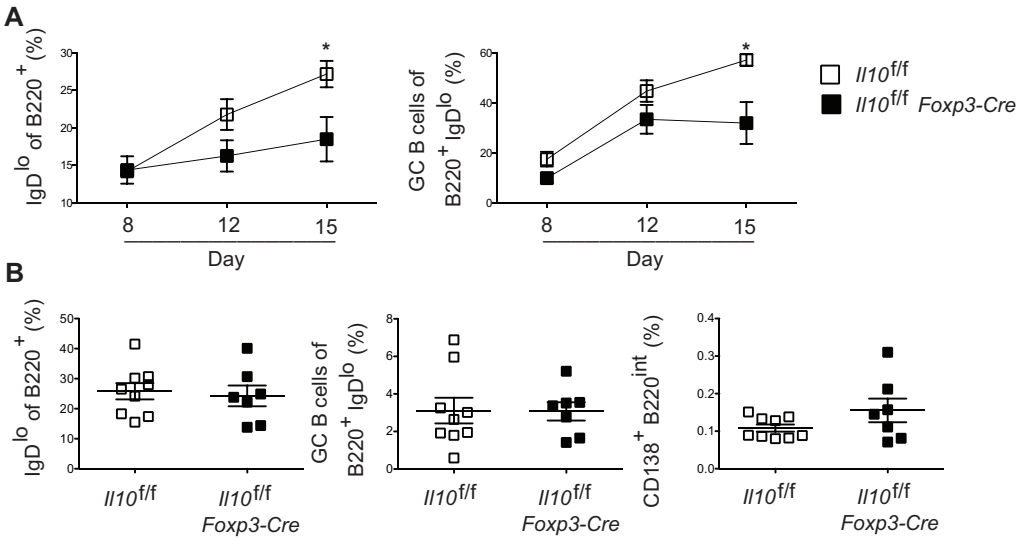

Figure S3. Temporal development of the GC B cell response in mice lacking regulatory CD4$^+$ T cell-derived IL-10. (**a**) Analysis of the B cell response in *Il10*$^{f/f}$ and *Il10*$^{f/f}$ *Foxp3*-Cre mice at days 8, 12, and 15 following LCMV infection. Frequency of activated and GC B cells as shown in gates in Figure S1b. Statistical analyses were performed using the unpaired two-tailed Student's *t*-test. (*, $p < 0.05$). Data are from one experiment representative of 3 experiments with 3-5 mice per group carried out 15 days and 3-4 experiments with 3-5 mice carried out at 8, 12, and 15 days following LCMV Armstrong infection. **(b)** Analysis of the B cell response in *Il10*$^{f/f}$ and *Il10*$^{f/f}$ *Foxp3*-Cre mice at day 15 following NP-OVA in complete Freund's adjuvant immunization. Frequency of activated, GC B cells and plasmablasts. Data are pooled from two experiments representative of 3 experiments with at 3-5 mice per group.

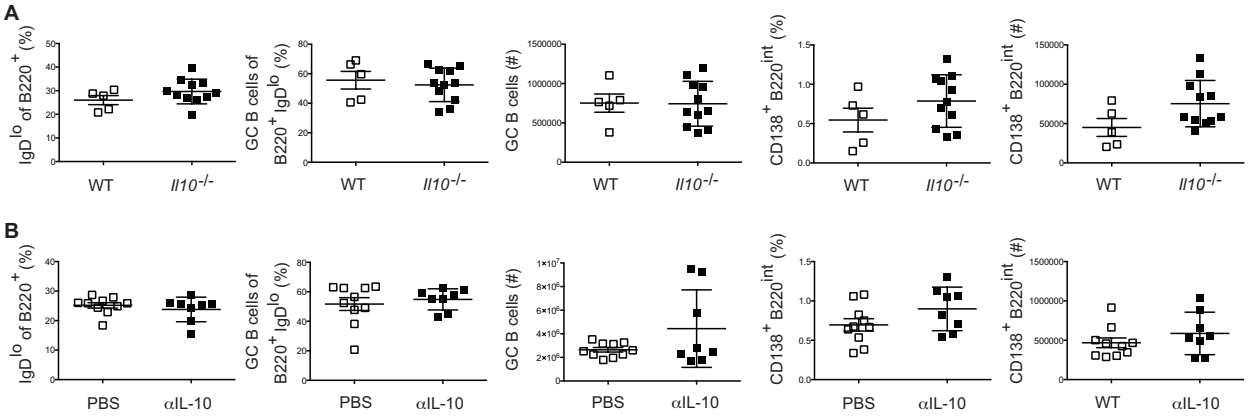

Figure S4. Systemic IL-10 is not required for the GC response. (**a**) Analysis of the germinal center response 15 days post acute LCMV-Armstrong infection in *Il10*$^{-/-}$ and control mice. Frequency and number of GC B cells and plasmablasts. Data are from 1 experiment representative of 3 experiments with 4-11 mice per group. (**b**) Analysis of the germinal center response 15 days post acute LCMV-Armstrong infection in mice treated with αIL-10 or PBS every other day beginning at day -1. Frequency and number of GC B cells and plasmablasts. Data are pooled from 2 independent experiments with 4-5 mice per group.

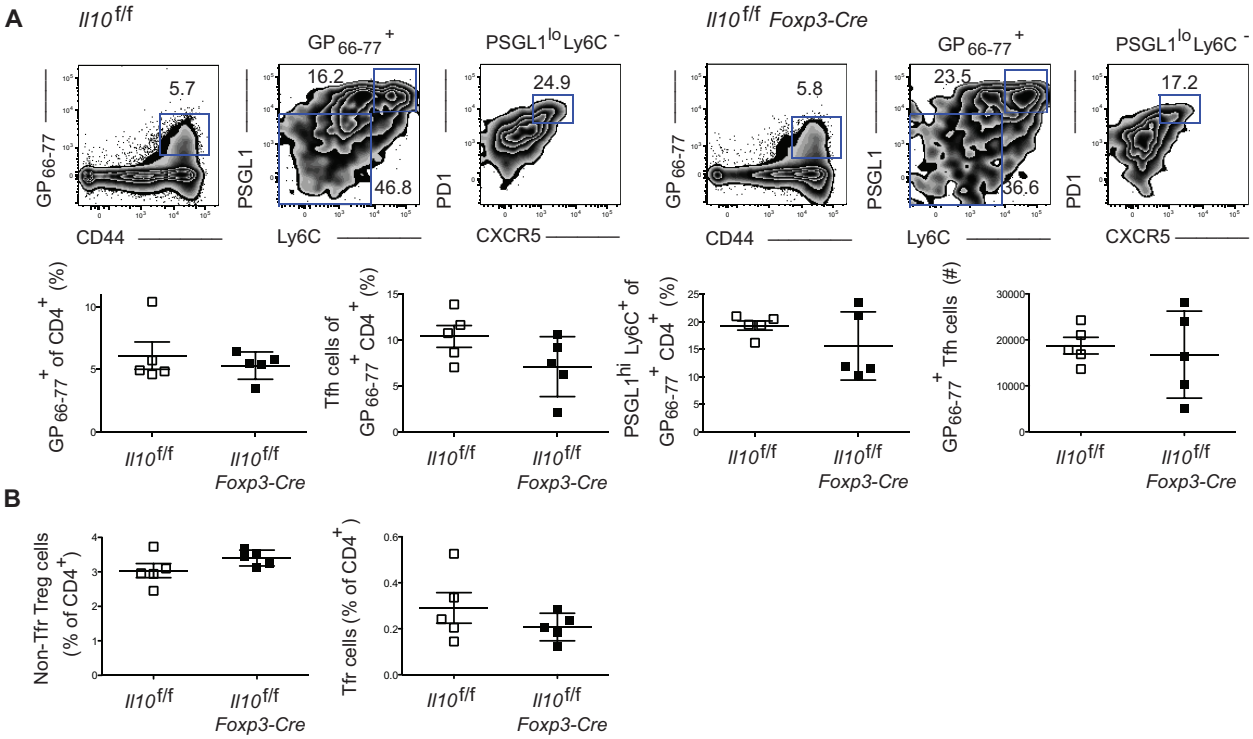

Figure S5. Regulatory CD4$^+$ T cell-derived IL-10 is not required for effector CD4+ T cell differentiation. Analysis of the CD4$^+$ T cell response in *Il10*$^{f/f}$ and *Il10*$^{f/f}$ *Foxp3*-Cre mice 8 days post LCMV infection. (**a**) Representative plots of the LCMV-specific CD4$^+$ T cell response. GP66$^+$ LCMV epitope specific CD4$^+$CD44$^+$ cells (top left) gated on Ly6C and PSGL1 (top middle). PSGL1^{lo}Ly6C$^-$ cells were further gated on CXCR5 and PD1 with the Tfh cell population defined by CXCR5 and PD1 expression (top right). Bottom: quantification of the results shown in the top plots. (**b**) Frequencies of Non-Tfr Treg cells (left) and Tfr cells (right). Data are from one experiment representative of 3 experiments with 3-6 mice per group carried out 8 days following LCMV Armstrong infection.

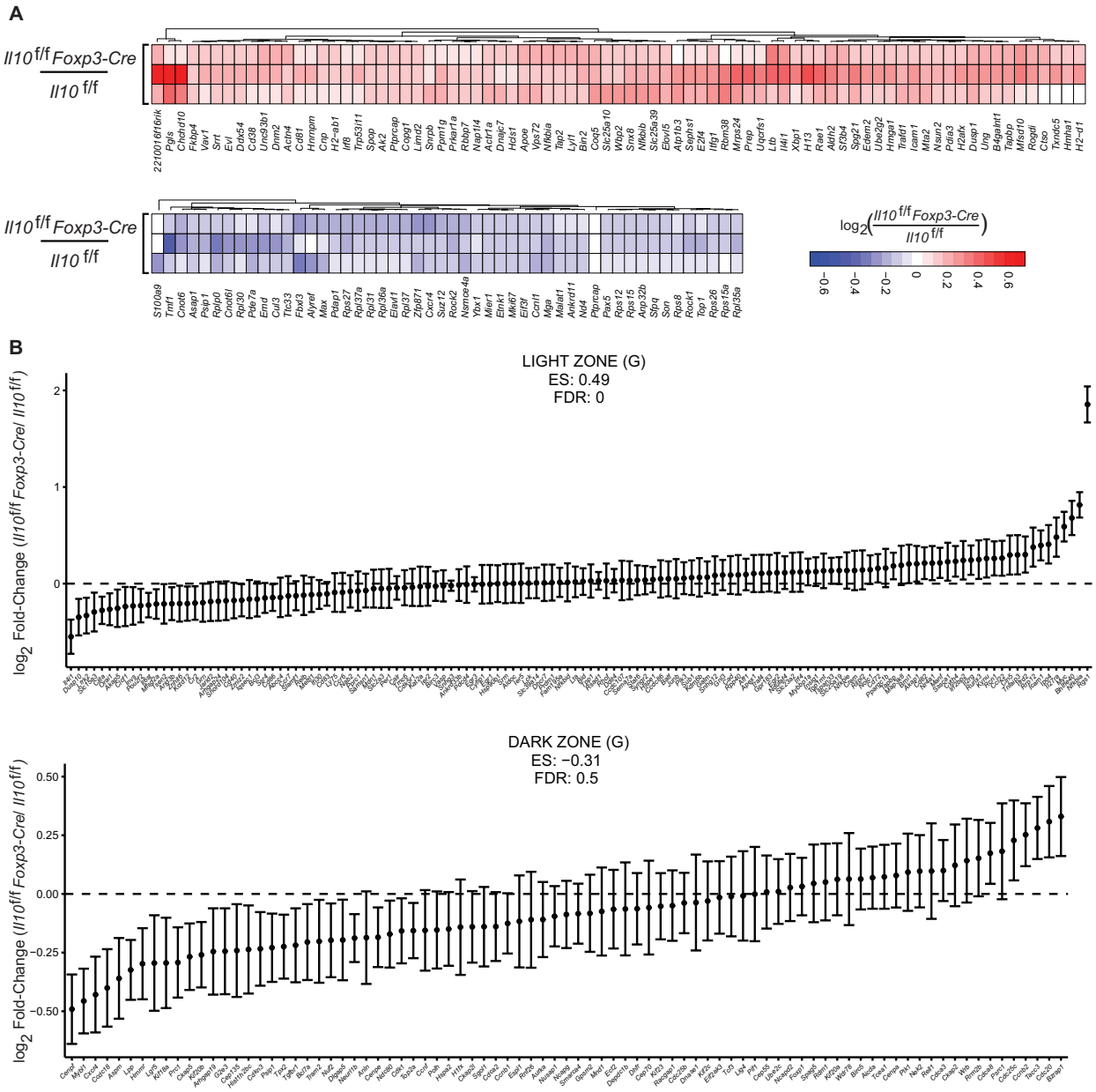

Figure S6. Heat map of DEGs based on RNA-seq. (a) Heat map of genes with a p-adjusted value < 0.1 (Benjami-Hochberg) and the corresponding $\log_2$ fold-change in mRNA isolated from GC B cells at 12 days post acute LCMV infection from *Il10*$^{f/f}$ and *Il10*$^{f/f}$ *Foxp3*-Cre mice. **(b)** GSEA of light zone versus dark zone signatures in GC B cells, based on published gene sets (*6*, *41*). Genes in light zone and dark zone gene sets with are shown with their corresponding expression (log2) in *Il10*$^{f/f}$ *Foxp3*-Cre cells relative to that in *Il10*$^{f/f}$ cells.

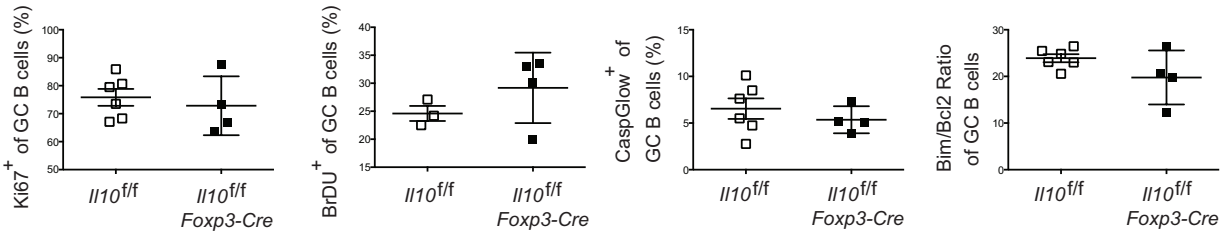

Figure S7. GC B cells in mice lacking regulatory CD4$^+$ T cell-derived IL-10 display similar levels of proliferation and death. Analysis of proliferation and cell death in GC B cells from *Il10*$^{f/f}$ and *Il10*$^{f/f}$ *Foxp3*-Cre mice 15 days post LCMV infection. Statistical analyses were performed using the paired two-tailed Student's *t*-test. Data are from one experiment representative of 2 experiments with at least 4 mice per group carried out 15 days following LCMV Armstrong infection.

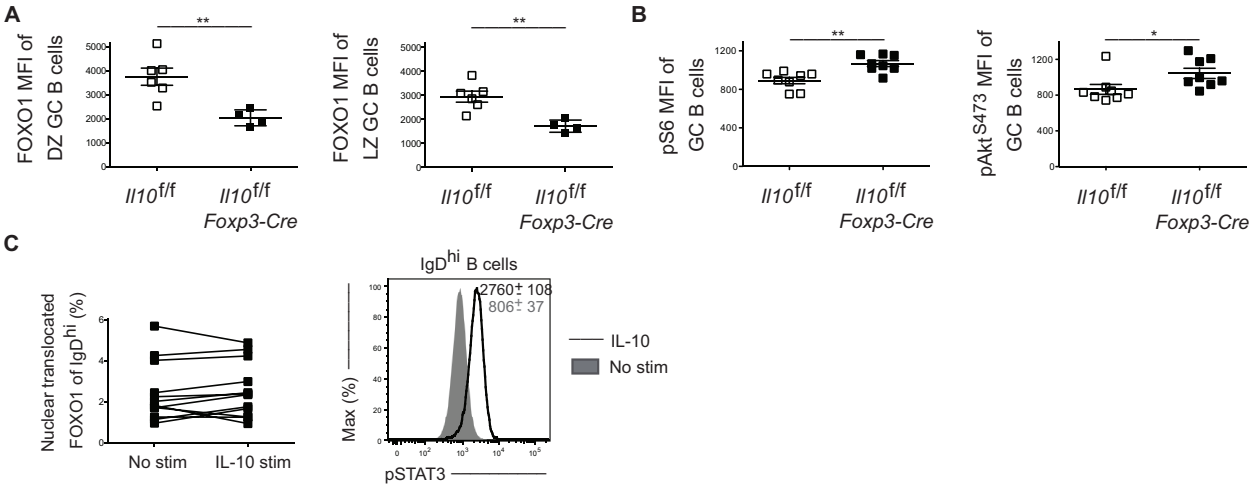

Figure S8. **IL-10 does not induce FOXO1 nuclear translocation in IgD^{hi} B cells.** (**a**) Expression of FOXO1 in dark zone and light zone GC B cells from *Il10*$^{f/f}$ or *Il10*$^{f/f}$ Foxp3-Cre mice 15 days after infection with LCMV. Data are from one experiment representative of 2 experiments with at least 4 mice per group carried out 15 days following LCMV Armstrong infection. Data are from one experiment representative of 2 experiments with at least 4 mice per group carried out 15 days following LCMV Armstrong infection. (**b**) Expression of phospho-S6 and phospho-Akt^{S473} in GC B cells from *Il10*$^{f/f}$ or *Il10*$^{f/f}$ Foxp3-Cre mice 15 days after infection with LCMV. Data are pooled from two experiments with 3-5 mice per group carried out 15 days following LCMV Armstrong infection. Statistical analyses were performed using the unpaired two-tailed Student's *t*-test. (*, $p < 0.05$; **, $p < 0.01$). (**c**) Assessment of the percentage of nuclear translocated FOXO1 following IL-10 stimulation in IgD^{hi} B cells 5 days post LCMV infection as determined by Amnis Imagestream (left). Analysis of phospho-STAT3 levels following IL-10 stimulation of IgD^{hi} B cells (right). Statistical analyses were performed using the paired two-tailed Student's *t*-test. Data are pooled from 3 experiments with 4 mice per group carried out 5 days following LCMV Armstrong infection.

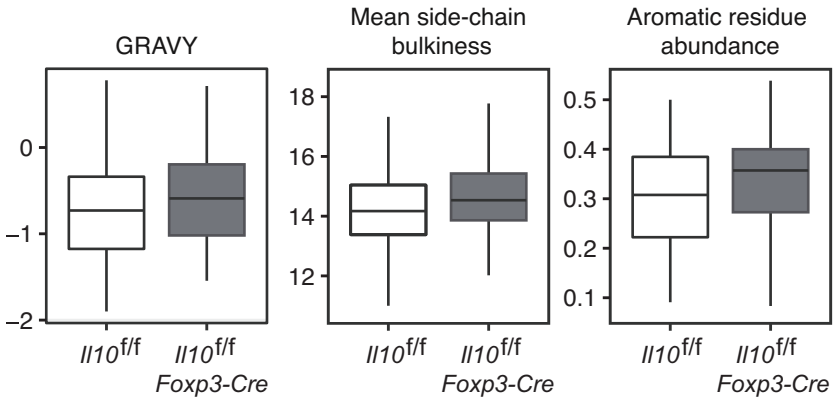

Figure S9. The V_H CDR3 region of GC B cells in mice lacking regulatory $CD4^+$ T cell-derived IL-10 displays altered amino acid physiochemical properties. Log_2 – fold-change of the V_H CDR3 physiochemical properties for *Il10*$^{f/f}$ or *Il10*$^{f/f}$ Foxp3-*Cre* mice 15 days after LCMV infection, including grand average of hydrophobicity (GRAVY) score, mean side-chain bulkiness and abundance of aromatic residues. Data are from 2 individual experiments pooled each with 3-5 mice per group.